Research in Pharmaceutical Sciences, October 2024; 19(5): 573-590
Received: 07-05-2024
Peer Reviewed: 05-06-2024
Revised: 16-07-2024
Accepted: 20-07-2024
Published: 22-10-2024

School of Pharmacy & Pharmaceutical Sciences
Isfahan University of Medical Sciences

Original Article

Novel SARS-COV2 poly epitope phage-based candidate vaccine and its immunogenicity

Sharareh Mohammad Hasani[1], Mahdi Behdani[2], Zohreh Amirkhani[1], Ilnaz Rahimmanesh[3], Mahsa Esmaeilifallah[1,4], Erfan Zaker[1,5], Parvaneh Nikpour[1], Mahmood Fadaie[1,5], Elham Ghafouri[1], Shamsi Naderi[1], and Hossein Khanahmad[1,*]

[1]*Department of Genetics and Molecular Biology, School of Medicine, Isfahan University of Medical Sciences, Isfahan, Iran.*
[2]*Department of Biotechnology, Biotechnology Research Center, Venom and Biotherapeutics Molecules Lab, Pasteur Institute of Iran, Tehran, Iran.*
[3]*Applied Physiology Research Center, Cardiovascular Research Institute, Isfahan University of Medical Sciences, Isfahan, Iran.*
[4]*Department of Parasitology and Mycology, School of Medicine, Isfahan University of Medical Sciences, Isfahan, Iran.*
[5]*Skin Diseases and Leishmaniasis Research Centre, Isfahan University of Medical Science, Isfahan, Iran.*

Abstract

Background and purpose: The global emergence of the severe acute respiratory syndrome coronavirus 2 (SARS-CoV-2) has prompted widespread concern. Bacteriophages have recently gained attention as a cost-effective and stable alternative for vaccine development due to their adjuvant properties. This study aimed to design and validate a poly epitope composed of viral proteins.

Experimental approach: SARS-CoV-2 proteins (spike, nucleocapsid, membrane, envelope, papain-like protease, and RNA-dependent RNA polymerase) were selected for analysis. Immunoinformatic methods were employed to predict B and T cell epitopes, assessing their antigenicity, allergenicity, and toxicity. Epitopes meeting criteria for high antigenicity, non-allergenicity, and non-toxicity were linked to form poly epitopes. These sequences were synthesized and cloned into pHEN4 plasmids to generate Poly1 and Poly2 phagemid vectors. Recombinant Poly1 and Poly2 phages were produced by transforming M13ΔIII plasmids and phagemid vectors into *E. coli TG1*. Female Balb/c mice were immunized with a cocktail of Poly1 and Poly2 phages, and their serum was collected for ELISA testing. Interferon-gamma (IFN-γ) testing was performed on spleen-derived lymphocytes to evaluate immune system activation.

Findings/Results: Recombinant Poly1 and Poly2 phages were produced, and their titer was determined as 10^{13} PFU/mL. Efficient humoral immune responses and cellular immunity activation in mice were achieved following phage administration.

Conclusion and implication: Poly epitopes displayed on phages exhibit adjuvant properties, enhancing humoral and cellular immunity in mice. This suggests that phages could serve as adjuvants to bolster immunity against SARS-Cov-2. Recombinant phages could be applied as effective candidates for injectable and oral vaccine development strategies.

Keywords: Coronavirus vaccines; Phage display; Poly epitopes; SARS-Cov-2.

INTRODUCTION

The severe acute respiratory syndrome coronavirus 2 (SARS-CoV-2)-related pandemic hit the world in December 2019. SARS-CoV-2 can infect the lungs and cause severe pathological damage, which the World Health Organization (WHO) has recognized (1). Many young adults may not display significant clinical symptoms; however, infections caused by SARS-CoV-2 in the elderly and those with underlying health conditions are more severe (2, 3).

*Corresponding author: H. Khanahmad
Tel/Fax: +98-3137929197
Email: h_khanahmad@med.mui.ac.ir, hossein_khanahmad@yahoo.com

Access this article online

Website: http://rps.mui.ac.ir

DOI: 10.4103/RPS.RPS_82_24

It is commonly accepted that more than 240 million verified instances of new coronavirus pneumonia, and the total number of deaths resulting from the disease has accumulated to more than 4 million around the globe. With the outbreak of SARS-CoV-2, major public health issues imposed significant financial burdens globally (4, 5). SARS-CoV-2 encodes replicase, spike protein, envelope protein, membrane protein, and nucleocapsid protein sequentially from genome 5' to 3' end (6).

Currently, there is a wide variety of vaccines available worldwide, including the BioNTech vaccine (manufactured by Pfizer Corp), mRNA vaccine (manufactured by Moderna Corp), AZD1222 adenovirus-based vaccine (manufactured by AstraZeneca Corp), JNJ-78436735 adenovirus-based vaccine (manufactured by Johnson & Johnson Corp), NVX-CoV2373 nanoparticle-based vaccine (manufactured by Novavax Corp), and others. Still, the appearance of SARS-CoV-2 variants has changed the epitopes of the original virus, which means that current may not be as effective (7). Given the mutable nature of SARS-CoV-2, it is imperative to accelerate the development of a highly effective SARS-CoV-2 vaccine to mitigate the spread of this highly contagious and severe illness (8).

Scientific evidence indicates that SARS-CoV-2 variants can evade the immune response triggered by the vaccine. Therefore, it is crucial to develop targeted vaccines against these viral mutants to prevent and control the SARS-CoV-2 pandemic eff. The development of vaccines globally utilizes a variety of technical approaches, with recombinant protein vaccines produced in vitro being the most widely used method (9).

The typical approach for designing a vaccine against acute viral infections involves inducing an immune response targeted at the virus. However, information regarding the SARS-CoV-2 virus is currently unavailable as it is unknown which specific parts of the virus (epitopes) are recognized by immune cells and whether they trigger an effective immune response. However, numerous initiatives have progressed to identify specific protein epitopes of SARS-CoV-2 that elicit T-cell responses (10). Identifying the specific epitopes and proteins of the virus recognized by T cells is essential for vaccine development. Most vaccine design approaches concentrate on spike proteins, and utilizing epitope design databases has proven to be highly advantageous in this domain (11). Multiple research groups are currently developing protein subunits for the new coronavirus vaccine. However, many of these groups have focused on selecting a particular protein subunit or only epitopes linking to cytotoxic T cells. Furthermore, alternative epitopes have not been thoroughly considered (12-14).

Phage display technology is a very efficient way of expressing foreign genomes that may be transferred. As previously stated, a key objective in vaccine development is to generate dominant immunological epitopes that can elicit robust immune responses. Consequently, using bacteriophage as a vaccination strategy has garnered the interest of several researchers, especially virologists. Phage-based vaccinations have not shown any significant adverse effects on the body, as seen from a scientific-practical standpoint (14). Bacteriophages are not regarded as human infectious agents and lack the potential to function as such. Moreover, the likelihood of bacteriophages binding to cell receptors and initiating cell signaling pathways is exceedingly low (15). Additionally, phages can stimulate both cellular and humoral immunity, which is a desired outcome for creating vaccines (16).

To develop a successful vaccine for this new virus, it is necessary to have a thorough understanding of antigen selection, immunogenicity methods, and appropriate animal models. Hence, employing alternative approaches like poly epitopes and phage display could shorten the timeline for vaccine development soon, while enabling the activation of various subtypes of immune cells and facilitating large-scale production. The objective of the present study was to create poly epitopes derived from essential structural proteins of the coronavirus, such as spike, envelope, membrane, nucleocapsid, RNA-dependent RNA polymerase (RDRP), and papain-like protease (PLP). The poly epitopes were displayed on the protein III of the M13

phage. Then, the ability of this genetically engineered vaccine to provoke an immune response in mice was examined. Our objective is to evaluate the capacity of these phages to serve as a framework for triggering immunological responses against the coronavirus.

MATERIAL AND METHODS

In-silico analysis

Identifying the SARS-CoV-2 target protein for poly epitope design and B and T cell epitope prediction

The protein sequences of spike, nucleocapsid, membrane, envelope, PLP, and RDRP from SARS-CoV-2 were retrieved from the Universal Protein Resource (UniProt) database (https://www.uniprot.org/). Subsequently, an exploration of B cell and T cell epitopes was conducted. Helper T cell epitopes were identified using the MHCPred tool (http://www.ddg-pharmfac.net/mhcpred/MHCPred/) (17), and the NetMHIICpan service (https://services.healthtech.dtu.dk/services/NetMHCIIpan-4.0/) (18), and Immune Epitope Database (IEDB) (http://tools.iedb.org/main/). Cytotoxic T-cell epitopes were determined through the NetMHCpan-4.1 service (https://services.healthtech.dtu.dk/services/NetMHCpan-4.1/) (18), and IEDB. B cell epitopes were ascertained utilizing the ABCpred tool (http://webs.iiitd.edu.in/raghava/abcpred/) (19), and BcePred (https://webs.iiitd.edu.in/raghava/bcepred/) (20), and IEDB. The antigenicity, allergenicity, and toxicity of consensus epitopes, were evaluated using data from at least two servers. The Helper T cell epitopes were developed using peptides containing 9 to 15 residues, the cytotoxic T cell epitopes containing 7 to 15 residues peptides, and the B cell epitopes containing peptides with 7 to 20 residues.

Analyzing the toxicity, immunogenicity, and antigenicity of selected epitopes

Antigenic epitopes were detected in Vaxijen 2.0 server (https://www.ddg-pharmfac.net/vaxijen/VaxiJen/VaxiJen.html) by targeting tumor cells and setting a threshold of ≥ 0.5 (21). Potential allergenic sites were assessed using the AlerTop (https://www.ddg-pharmfac.net/AllerTOP/) (22). Finally, to prevent possible toxicity, the epitopes were analyzed using default support vector machine parameters in the ToxinPred service (https://webs.iiitd.edu.in/raghava/toxinpred/protein.php) (23).

Predicting secondary structure

The Protein Structure Prediction Server (PSIPRED) (http://bioinf.cs.ucl.ac.uk/psipred/) online program was used to generate the secondary structure of the intended vaccine construct. PSIPRED is a top-rated service that has been utilized to predict the secondary structure of the protein. The server employs two feed-forward neural networks to accurately assess the protein output given by a position-specific iterated basic local alignment search tool (PSI-BLAST). Throughout the analysis, all server parameters remained unchanged, adhering to their default values (24).

Estimation of physicochemical properties of poly epitope and tertiary structure

Linkers were employed to establish connections between distinct epitopes, with GPGPG utilized for linking helper T cell epitopes, AAY for cytotoxic T cell epitopes, and KK for B cell epitopes. Subsequently, the physicochemical properties of the identified epitopes were forecasted using ProtParam (https://web.expasy.org/protparam/) (25). The probable three-dimensional structure of the poly epitope was modeled using the Iterative Threading ASSEmbly Refinement (I-TASSER) server (https://zhanggroup.org/I-TASSER/) (26).

Refinement and validation of tertiary structure

The GalaxyRefine Server (http://galaxy.seoklab.org/cgi-bin/submit.cgi?type=REFINE) (27) was employed to enhance the accuracy of the projected tertiary structures. GalaxyRefine utilizes iterative optimization techniques and multiple geometric operators to increase the precision of the basic models. The final refined models were assessed to evaluate their tertiary structures using the Structure Analysis and Verification (SAVES 6.1) server (https://saves.mbi.ucla.edu/). The SAVE server provides the Ramachandran plot for the entire

structure, evaluates the overall quality of the tertiary structure, and computes various parameters such as buried protein atoms, stereochemical quality, and atomic interactions of the anticipated 3D structure.

Peptide-protein docking

We utilized the GalaxyPepDock peptide-protein flexible docking service (http://galaxy.seoklab.org/cgi-bin/submit.cgi?type=PEPDOCK) to assess the development of the major histocompatibility complex (MHC)-peptide complex (28). This study demonstrates the application of GalaxyPepDock to individually analyze epitopes and Protein Data Bank (PDB) files of mouse MHC alleles.

In silico cloning optimization

The protein sequence underwent reverse translation into DNA sequences utilizing the sequence manipulation suite (SMS) tool (https://www.bioinformatics.org/sms2/rev_trans.html/) (29). Subsequently, the JCat tool (http://www.jcat.de/) (30), was employed to optimize the DNA sequences, considering *E. coli* codon usage bias, with the aim of achieving elevated levels of protein production. Finally, a production order was initiated for the cloning process into the pHEN4 vector, and this procedure was entrusted to the GeneCust firm.

In-vitro studies

Production of E. coli TG1 containing pHEN4-Poly1 and pM13ΔpIII, and E. coli TG1 containing pHEN4-Poly2 and pM13ΔpIII

Phage display systems, such as M13KO7d3, use defective helper phages to increase the number of binding sites and improve the effectiveness of the screening process. These systems facilitate the display of peptides and proteins on the pIII protein of the phage (31). In this study, M13KO7 plasmids containing pM13ΔpIII were used. The poly-epitope fragment is subdivided through polymerase chain reaction (PCR) reactions involving two pairs of specific primers (Table S1 available at: https://github.com/supplement-R/supplementary), executed on the phagemid vector provided by GeneCust Company. Consequently, the fragment was divided into two distinct entities, Poly1 and Poly2, each comprising approximately 800 nucleotides. Subsequently, the Poly1 and Poly2 genes were subjected to cleavage through *SalI* and XbaI restriction enzymes. Simultaneously, the pHEN4 plasmid characterized by alterations in its multiple cloning sites containing the recognition sites for the described enzymes was cleaved. After these enzymatic processes, a ligation reaction ensued between the resultant insert and the modified vector.

Employing the conventional $CaCl_2$ technique, the pHEN4-Poly1 vector and pHEN4-Poly2 were independently transformed into *E. coli TOPO10* (32, 33). After the transformation, colony PCR using specific primers was performed to confirm the successful incorporation, followed by plasmid extraction from the validated colonies. The extracted plasmids were then transformed into *E. coli TG1*. Lastly, the pM13ΔIII plasmids were transformed into *E. coli TG1*, incorporating both pHEN4-Poly1 and pHEN4-Poly2 vectors that had undergone prior transformation. Transformed bacteria were selected based on Luria-Bertani (LB) agar plates containing 50 µg/mL kanamycin and 100 µg/mL ampicillin. To validate the insertion of the plasmid into the TG1 harboring pHEN4-Poly1/2 and pM13ΔIII, colony PCR was employed utilizing M13KO7 and pHEN primers, as detailed in Table S1 (available at: https://github.com/supplement-R/supplementary).

Production of Poly1 and Poly2 recombinant phages

Employing a 0.22-µ filter and a 20% polyethylene glycol-NaCl solution, the phage was harvested from 1-L Erlenmeyer flask (25% working volume) using super broth medium (35 g/L peptone, 20 g/L yeast extract, and 5 g/L NaCl, containing 50 µg/mL kanamycin and 100 µg/mL ampicillin) containing *E. coli TG1* harboring pHEN4-Poly1 and pM13ΔIII, as well as *E. coli TG1* harboring pHEN4-Poly2 and pM13ΔIII plasmids. The cultures were incubated at 37 °C with shaking at 200 rpm for 12-16 h to facilitate bacterial growth and phage production. Subsequently, this was followed by resuspending the pellet in phosphate-buffered saline buffer and titrating it using serial dilution procedures.

Verification of produced phage by enzyme-linked immunosorbent assay

At first, 10 µL of every phage sample was combined with 90 µL of coating buffer and applied to each well of a 96-well enzyme-linked immunosorbent assay (ELISA) plate to coat the phages as antigens. After three washes, the plate wells were filled with 200 µL of 5% skim milk and kept at 37 ℃ for 1 h. After three washes, 100 µL of anti-M13 antibody P III - horseradish peroxidase (HRP) conjugate (Sino Biological, China) solution was added to wells at a dilution of 1:2000 and incubated at room temperature for 1 h. Following three washes, 100 µL of tetramethylbenzidine solution was added, resulting in a blue color after 15-20 min. The reaction was stopped using 50 µL of stop solution, and the optical density (OD) was measured at a wavelength of 450 nm.

Tittering of the phage

The tittering process for the produced phages was conducted following the guidelines. In summary, serial dilutions (10-fold) of the phages were prepared, and 10 µL of each dilution was mixed with 200 µL of mid-log phase *E. coli TG1* cells. The resulting mixture was added to 1 mL of prewarmed top agar and spread evenly onto prewarmed LB plates. Following a brief cooling period at 4 °C for 5 min, the plates were inverted and then incubated at 37 °C overnight. Subsequently, the phage plaques were enumerated, and the titers were determined based on the plaque counts and their corresponding dilutions.

In-vivo studies

Mice immunization using recombinant phage

Two distinct groups, each comprising three subgroups with six BALB/c female mice per subgroup (6-8 weeks), obtained from the Pasteur Institute of Iran, were employed for the study. The study received approval from the Ethics Committee of Isfahan University of Medical Sciences in Isfahan, Iran (Ethic Code: IR.MUI.MED.REC.1399.226). The mice were subjected to a 12/12-h light/dark cycle, maintained at a temperature of 22 °C with a humidity level of 55%. They were provided with unrestricted access to water and food. The administration protocol involved subcutaneous injection for the first group and gavage for the second group. Within each group, the first subgroup received 5×10^{10} Poly1 and 5×10^{10} Poly2 phage vaccine particles, the second subgroup received 10^{11} helper phage particles, and the third subgroup received PBS, respectively (Fig. 1).

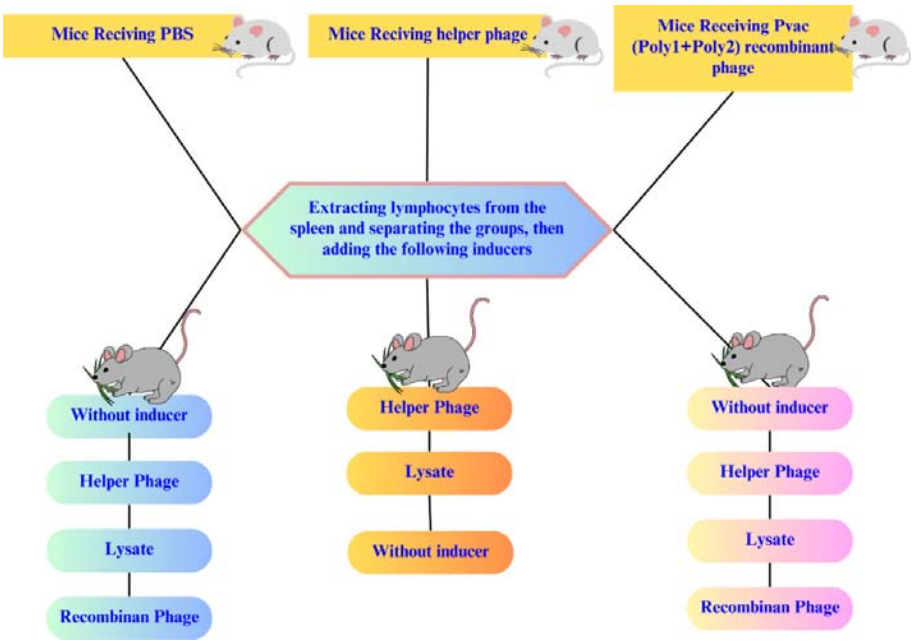

Fig. 1. Schematic image of the grouping of mice and the number and type of inducers used during the cellular immune assessment.

Assessing humoral immune response

The interaction between vaccine phages and mice serum antibodies was evaluated using ELISA. Specifically, 5 µL of 10^{10} Poly1 and Poly2 vaccine phage particles with 90 µL of coating buffer, were dispensed into the first set of 6-µL plates for each group. The second set of six wells received 10 µL of 10^{11} helper phage particles and 90 µL of coating buffer. In the third set of six wells, 100 µL of coating buffer devoid of phages, and an additional 100 µL of lysate (Commercially available SARS-CoV-2 vaccines, including PastoCovac, CovIran Barekat, Sinopharm, and Sputnik V, were utilized to generate a lysate preparation. A pooled aliquot of these vaccines was subjected to the concentrate using a vacuum evaporator for about 4 h, resulting in the ready lysate) being introduced into the fourth set of six wells. Subsequently, the plates were stored overnight at 4 °C. The subsequent steps involved a wash and blocking phase using 5% skim milk. Following additional washes, the first set of six wells (receiving phage vaccine), the second set of six wells (receiving helper phage), the third set of six wells (receiving PBS), and the fourth set of six wells (Lysate) were supplemented with mouse sera. These wells underwent incubation and subsequent washes. The anti-mouse immunoglobulin-HRP conjugate (IgG; Cyto Matin Gene, Iran) was then introduced, and after incubation, each well received 100 µL of BD Biosciences' tetramethylbenzidine substrate reagent. This mixture was incubated for 18 min at room temperature. Absorbances were measured at 450 nm using an automatic ELISA reader (Bio-Rad, California, USA) after adding 50 µL of chromogenic termination with 2 M H_2SO_4.

Assessing cellular immune response

In order to measure the level of interferon-gamma (IFN-γ) production, which serves as an indirect indicator of cellular immune activation, it was determined that the spleen would be isolated from the mice in each group, cultured, and stimulated. In this experiment, cultivation was conducted using 48 plates. After 48 h of induction with either helper or recombinant phage, as well as PBS and lysate from all groups, the supernatant of the culture medium was collected and subjected to centrifugation at 1500 rpm for 5 min. Subsequently, the samples were sent to Karmania Pars-Gen, Iran, to measure IFN-γ.

Statistical analysis

The statistical analysis was conducted using the GraphPad Prism Software Version 10 (Computer software, San Diego, CA). The One-way ANOVA multiple components test followed by Tukey post-hoc test and independent t-test was employed to compare the treatment groups in both *in-vivo* and *ex-vivo* experiments. *P*-values ≤ were considered statistically significant.

RESULTS

Specific selected B and T cell epitopes and their immunogenicity, toxicity, and allergenicity

After identifying the shared epitopes throughout the databases, the antigenicity, allergenicity, and toxicity of the shared epitopes were assessed using VaxiJen, AllerTop, and ToxinPred databases. Candidates included 41 epitopes with the highest antigenicity score that were not toxic or allergens (Table 1).

Poly epitope construct and its physicochemical properties

The chosen epitopes were joined to one another using the proper linkers. The poly epitope with better stability was chosen after thoroughly analyzing its antigenicity, allergenicity, toxicity, and physicochemical properties (Table 2 and Fig. 2). The potential immune responses of predicted epitopes were evaluated using the VaxiJen score, based on epitopes' physicochemical properties. Poly1 had a moderate antigenicity score of 0.6782, and Poly2 scored 0.5579. Both epitopes assessed for allergenicity and toxicity using Alertop and ToxinPred were found to be non-allergenic and non-toxic, suggesting they are good candidates for further vaccine development. Poly1 has a molecular weight of 29,325.35 Da, and Poly2 is slightly heavier at 30,100.56 Da. Stability tests showed Poly1 has a half-life of 1.9 h in mammalian systems, over 20 h in yeast, and 10 h in *E. coli*. Poly2 has a 20-h half-life in mammalian reticulocytes and 30 min in yeast but over 10 h in *E. coli*.

Table 1. Candidate B and T cell epitopes.

Sequence	Cell type	Protein	Antigenicity
SYLTPGDSS	B	S1	0.7499
TTLDSKTQ	B	S1	1.0912
YAWNRKRI	B	S1	0.7206
GVLTESNK	B	S1	0.7779
VYFASTEK	B	S1	0.9206
NNLDSKV	B	S1	0.5082
GAAAYYVGY	T (MHCII-CD4)	S1	0.6604
QSLLIVNNATNVVIK	T (MHCII-CD4)	S1	0.8082
MFVFLVLLPLVSSQ	T (MHCII-CD4)	S1	0.8022
ATRFASV	CTL (MHCI-CD8)	S1	0.8830
IAVEQDKNT	B	S2	0.6823
LPVSMTK	B	S2	0.8810
IPTNFTISV	T (MHCII-CD4)	S2	0.8820
VLPFNDGVY	CTL (MHCI-CD8)	S1S2	0.6642
FNATRFASV	T (MHCII-CD4)	S1S2	0.6609
FNAEIRASANL	CTL (MHCI-CD8)	S1S2	0.7082
STECSNLLL	CTL (MHCI-CD8)	S1S2	0.5871
VTTEILPV	CTL (MHCI-CD8)	S1S2	0.8441
IPTNFTISV	T (MHCII-CD4)	S1S2	0.8241
GMSRIGMEV	CTL (MHCI-CD8)	N	0.6287
GARSKQRRP	B	N	0.8316
SAAEASKKPRQKRTA	B	N	0.8326
NQLESKMSGKGQQ	B	N	0.8227
QALPQRQKKQ	B	N	0.8320
ISAKNRA	B	RDRP	2.3024
LYVKPGGTSSGD	B	RDRP	0.7788
LQPEEEQE	B	PLP	0.8501
VKPTVVVNA	B	PLP	0.7888
AGIFGADPIHSLRV	B	PLP	08088
IVEEA	B	PLP	0.7988
SRVKNLNSSRV	B	E	0.8506
SFVSEET	B	E	0.7302
YVYSRVKNL	CTL (MHCI-CD8)	E	0.7020
VLLFLAFVV	CTL (MHCI-CD8)	E	0.5977
NIVNVSLVK	CTL (MHCI-CD8)	E	0.9310
KPSFYVYSRVKNLNS	T (MHCII-CD4)	E	0.8229
VKPSFYVYSRVKNLN	T (MHCII-CD4)	E	1.2319
SFYVYSRVKNLNSSR	T (MHCII-CD4)	E	0.6291
PLLESELVIGAVILRGHLRI	B	M	0.6678
LLWPVTLA	B	M	0.8900

S, Spike; N, nucleocapsid; M, membrane; E, envelope; PLP, papain-like protease; RDRP, RNA-dependent RNA polymerase.

Poly2 is likely more stable than Poly1, indicated by a lower instability index (28.05 *vs* 47.79) and a higher aliphatic index (87.28 *vs* 64.26), suggesting better thermostability. The grand average of the hydropathy index showed that Poly1 is hydrophilic (-1.278) and Poly2 is slightly hydrophobic (0.149), affecting their solubility.

Table 2. Characteristics and physicochemical properties of the poly epitopes.

Vaccine	VaxiJen score	AlerTop	Toxicity	Molecular weight (Da)	Half life	Instability index	Aliphatic index	Gravity
Poly 1	0.6782	Non-allergen	Non-toxic	29325.35	1.9 h (mammalian) > 20 h (yeast, *in vivo*). > 10 h (*E. coli, in vivo*)	47.79	64.26	-1.278
Poly 2	0.5579	Non-allergen	Non-toxic	30100.56	20 h (mammalian reticulocytes, *in vitro*) 30 min (yeast, *in vivo*) > 10 h (*E. coli, in vivo*)	28.05	87.28	0.149

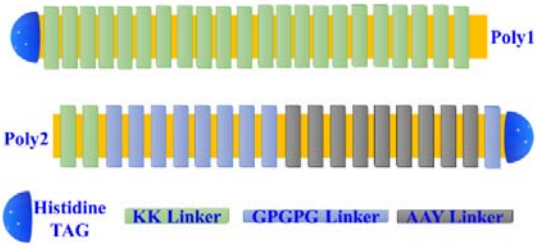

Fig. 2. The schematic representation of the epitope construct, assembled from SARS-CoV-2 proteins connected by linkers.

Predicting secondary structure

PSIPRED was used to determine the secondary structures of alpha-helices, beta-strands, and random coils. The PSIPRED server predicted the presence of 51.16% alpha-helices, 4.65% β-strands, and 44.19% random coils for Poly1 and 29.96% alpha-helices, 25.17% β-strands, and 44.87% random coils for Poly2 (Fig. 1S available at: https://github.com/supplement-R/ supplementary).

Refinement and validation of tertiary structure

The model predicted by I-TASSER (Fig. 3A and C) was further revised using the Galaxy Refine service. Among the five refined models developed, model 1 was selected for further investigation due to its superior quality compared to the raw model (Fig. 3B and D). This choice was based on its lowest root-mean-square deviation (RSMD) score (0.403 and 0.395), global distance test - high accuracy (GDT-HA) score (0.9545 and 0.9583), MolProbity score (2.270 and 2.748), and a Rama preferred region of 82.4 and 79.6, respectively for Poly1 and Poly2. The protein structure was confirmed using Ramachandran plot analysis by the PROCHECK server. The results indicate that 71.7% and 71.5% of the residues are located in the most preferred region, respectively, 20.2% and 23.2% in the extra authorized region, 1.7% and 1.8% in generously allowed regions, and 6.4% and 3.5% in the banned region, as depicted in Fig. 4A and B. The ERRRAT server reported that the final model had an overall quality factor of 77.2 and 41.02 for Poly1 and Poly2, respectively.

Peptide-protein docking

Flexible docking of peptides to proteins

The initial step involved downloading the available structural data of MHC-I and MHC-II from the PDB (RCSB PDB) server. The server received the epitopes and MHC PDB files as independent submissions. Subsequently, the top models, that exhibited the highest interaction similarity scores were selected for each peptide and its MHC. The interaction similarity score quantifies the resemblance between the amino acids of the target complex and the contacting residues in the template structure, which is obtained from the GalexyPepDock server. Overall, cytotoxic T-lymphocyte (CTL) epitopes exhibited superior docking quality compared to T helper cell epitopes (Table 3).

pHEN4-Poly1 and pHEN4-Poly2 recombinant vector construction

The pHEN4-Poly1 and pHEN4-Poly2 constructs were effectively produced by enzymatically digesting the pHEN4 plasmid (Fig. 2S available at: https://github.com/supplement-R/supplementary) and the matching Poly1 and Poly2 fragments obtained from PCR amplification. The enzymatic activity, aided by *SalI* and *XbaI* enzymes (Fig. 3S available at: https://github.com/supplement-R/supplementary), efficiently split the plasmid and fragments into their components, establishing the foundation for further assembly.

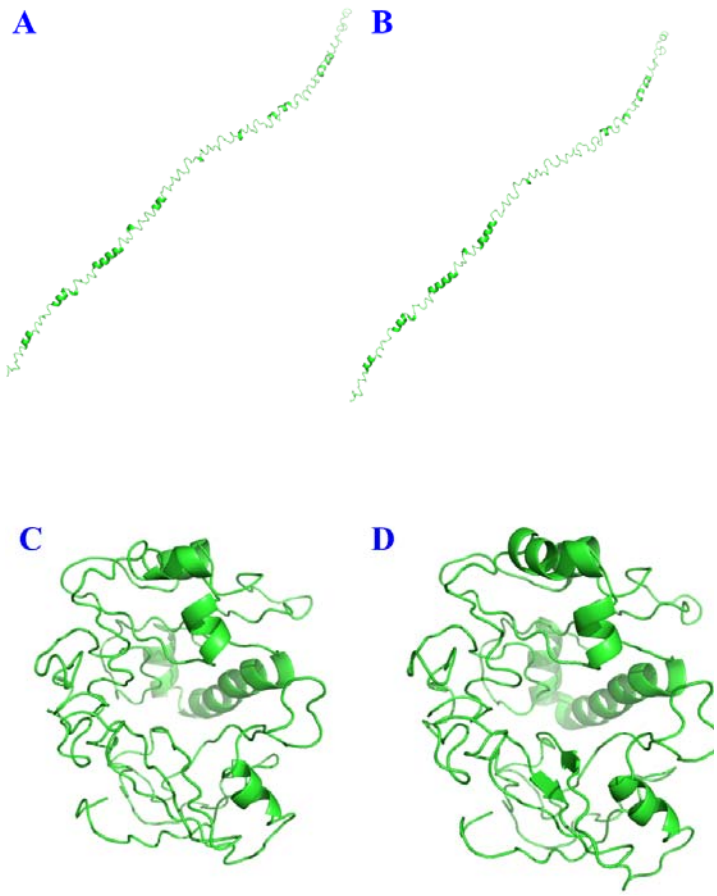

Fig. 3. The tertiary structures of poly 1 and poly 2 are shown in A and B for poly 1, and in C and D for poly 2. A and C represent the structures predicted by I-TASSER, while B and D depict the refined structures obtained through GalaxyRefine.

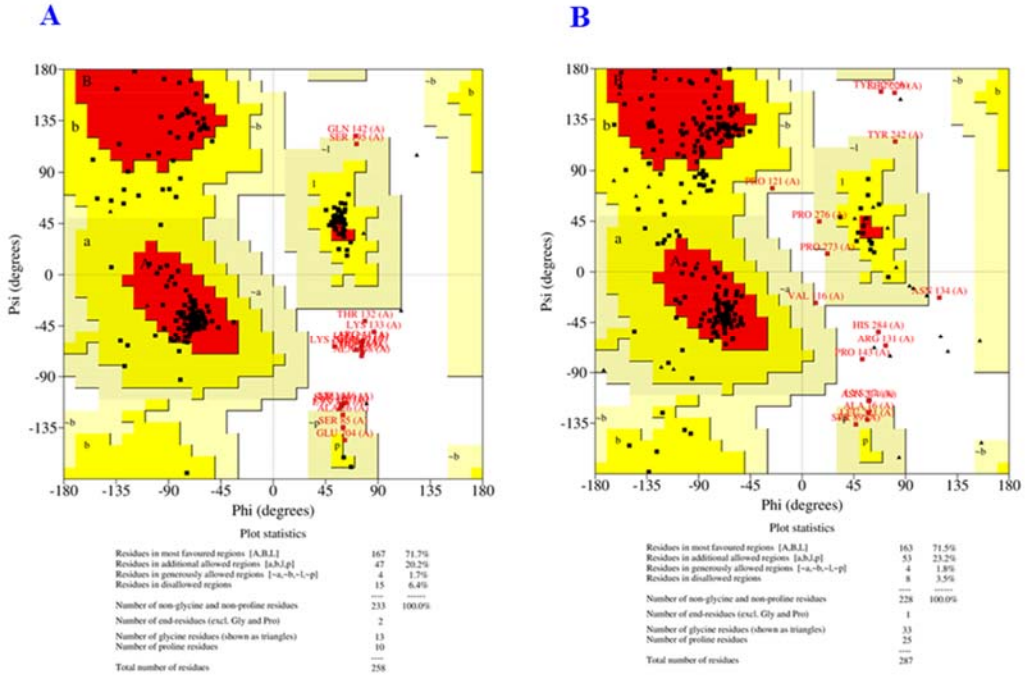

Fig. 4. Ramachandran plot of (A) Poly1 and (B) Poly2 proteins.

Table 3. Interaction similarity scores of the adopted cytotoxic T-lymphocyte and T helper epitopes were determined using the GalexyPepDock flexible docking server. Numbers are based on interaction similarity scores

Mouse MHC Class I				Mouse MHC Class II	
Sequence	**H2-Dd**	**H2-Kd**	**H2-Id**	**Sequence**	**I-Ad**
STECSNLLL	225	228	314	GAAAYYVGY	119
FNATRFASV	251	308	310	QSLLIVNNATNVVIK	98
VLLFLAFVV	220	261	292	VKPSFYVYSRVKNLN	141
YVYSRVKNL	210	221	282	IPTNFTISV	103
NIVNVSLVK	171	178	256	SFYVYSRVKNLNSSR	118
VLPFNDGVY	198	225	295	MFVFLVLLPLVSSQ	111
VTTEILPV	166	174	235	KPSFYVYSRVKNLNS	123
AEIRASANL	201	279	362		
ATRFASV	136	192	244		

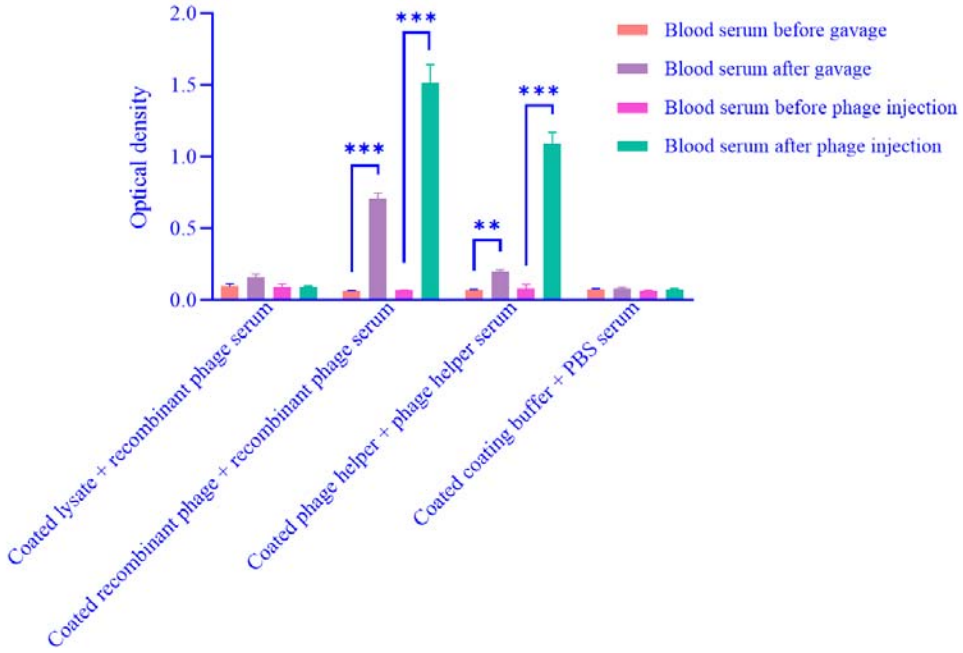

Fig. 5. Optical densities of the mice sera at 450 nm wavelength. The optical density observed in the two groups of mice, one provided *via* gavage and the other *via* subcutaneous injection, are displayed in a side-by-side comparison. The data is presented as mean ± SD. $^{**}P \leq 0.01$ and $^{***}P \leq 0.001$ indicate significant differences between groups. PBS; Phosphate buffered saline.

Transformation to E. coli TOP10

After confirming the development of colonies using colony PCR, plasmids were isolated from the verified colonies and subsequently introduced into *E. coli* TG1 cells, as shown in Fig. 4S (available at: https://github.com/ supplement-R/supplementary).

Co-transformation of E. coli TG1 containing pHEN4-Poly1 or Poly2 with pM13ΔIII and colony PCR verification

The pM13ΔIII plasmids were transformed into two strains of *E. coli TG1*, one having pHEN4-Poly1 and the other containing pHEN4-Poly2. The bacteria were then grown on LB agar plates that had been treated with both ampicillin and kanamycin. Colony PCR was performed using particular primers to confirm the growth of colonies (Fig. 5S available at: https://github.com/supplement-R/supplementary).

Producing phages and titration

After the phages were purified, the serial dilution procedure was used to calculate the phage titer. The phage titer, quantified at 10^13, was determined utilizing a serial dilution method.

Phage verification

Transduction was used to introduce the recombinant Poly1 and Poly2 phage into *E. Coli TG1*. To verify the lack of *E. coli TG1* bacterium contamination, we cultivated empty *E. coli TG1* on LB agar media supplemented with ampicillin and kanamycin. An ELISA was conducted employing an antibody specific to the M13 bacteriophage. The disparity in light absorption at a wavelength of 450 nm between the phage samples and the coated buffer signifies the existence of phage. Statistical analysis is not possible due to the limited sample size. Thus, it can be assumed that the anti-M13 antibodies are connected with the produced phages. This conclusion is based on the fact that the only protein expressed in the bacteria is specifically linked to the recombinant phagemid protein three. Consequently, it can be affirmed that Poly1 and Poly2 are displayed on the surface of phage protein III (Table S3 available at: https://github.com/supplement-R/supplementary).

Assessing humoral immunity

The previously described procedure was followed for the ELISA steps to determine whether the mice's serum contained antibodies against phages. The PBS subgroup's optical absorbance was similar before and after gavage and subcutaneous injection. The coated lysate subgroup did not have significant differences in serum optical absorbance following recombinant phage delivery in both methods. The phage helper subgroup showed significant differences in serum optical absorbance after both treatment routes (mouse serum received gavage and subcutaneous injection). The recombinant phage subgroup exhibited significant increase in serum OD following both route of administration (Fig. 5).

Assessing cellular immunity

The IFN-γ (pg/mL) levels were assessed in mice under various treatments, as shown in Fig. 6. As shown in Fig. 6A, subcutaneous administration of PBS, helper phage, and recombinant phage showed significantly higher IFN-γ levels in the helper phage group than others.

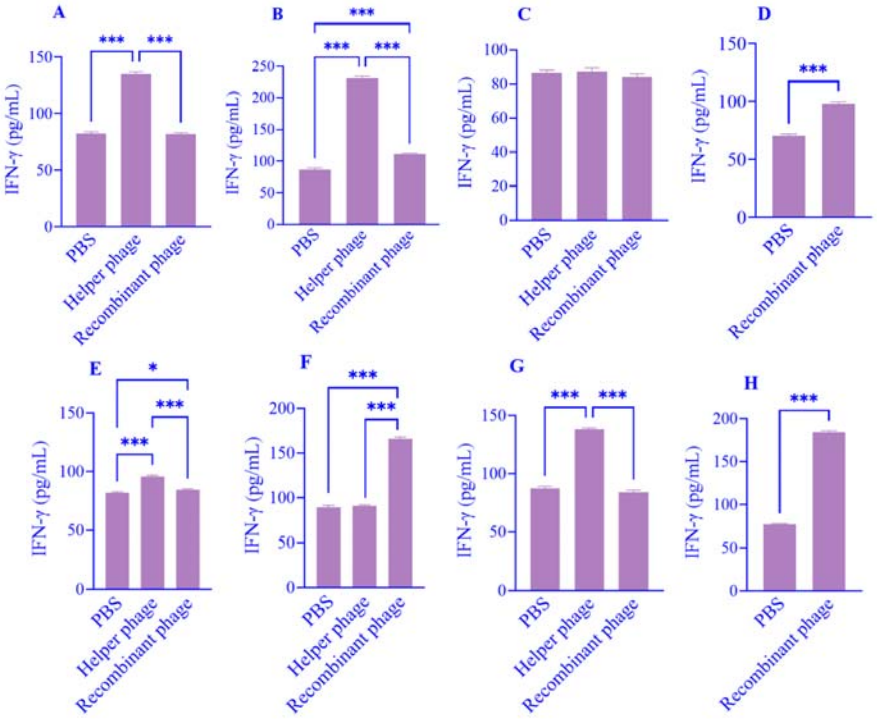

Fig. 6. IFN-γ production was assessed in response to different treatments. The levels of IFN-γ in mice subjected to various treatments were measured across different experimental groups. IFN-γ levels in mice treated subcutaneously with (A) PBS, helper phage, and recombinant phage and lymphocytes did not receive any inducer; (B) PBS, helper phage, and recombinant phage and lymphocytes treated with helper phage; (C) PBS, helper phage, and recombinant phage and lymphocytes received vaccine lysates; (D) PBS and recombinant phage and lymphocytes received recombinant poly epitopes. (E) IFN-γ levels in mice treated *via* gavage with PBS, helper phage, and recombinant phage and lymphocytes did not receive any inducer; (F) PBS, helper phage, and recombinant phage and lymphocytes received helper phage; (G) PBS, helper phage, and recombinant phage and lymphocytes received vaccine lysates. (H) Gavage recombinant: IFN-γ levels in mice treated *via* gavage with PBS and recombinant phage and lymphocytes received recombinant poly epitopes. *$P \leq 0.05$, **$P \leq 0.01$, and ***$P \leq 0.001$ indicate significant differences between groups. IFN-γ, Interferon gamma; BPS, phosphate buffered saline.

Lymphocytes, treated with helper phage, demonstrated a similar trend in which the groups treated with helper phage showed the highest IFN-γ levels and the recombinant phage group also had significantly higher IFN-γ levels compared to PBS (Fig. 6B). Results in Fig. 6C (lymphocytes received vaccine lysates) display no significant differences among different treatment groups. It was revealed that recombinant poly epitopes significantly increased IFN-γ levels compared to PBS (Fig. 6D). In Fig. 6E, gavage administration without an inducer highlighted significantly higher IFN-γ levels in the helper phage group and a notable increase in the recombinant phage group compared to PBS. IFN-γ levels in the recombinant phage group were notably higher than the other two groups when lymphocytes received helper phage (Fig. 6F). Gavage administration and lymphocytes received vaccine lysates, resulted in a considerably higher IFN-γ levels in the helper phage group (Fig. 6G). Gavage administration and lymphocytes received recombinant poly epitopes led to a significantly higher IFN-γ level in the recombinant phage group than in the PBS-treated group (Fig. 6H).

DISCUSSION

SARS-CoV-2 infections have disseminated globally and have swiftly emerged as a significant public health concern impacting many age cohorts. There is a pressing need to develop targeted prevention and therapies, such as vaccination and medication candidates for this condition. Immunoinformatic methodologies are economically efficient, aiding researchers in forecasting antigenic and immunogenic epitopes necessary for developing epitope-based vaccines against any pathogen (34, 35). This study aimed to use an integrated strategy to create a low-cost, safe vaccination against SARS-CoV-2. In the current study epitopes of protein spike along with the epitopes of envelope, membrane, nucleocapsid, PLP, and RDRP proteins were used to construct this vaccine to achieve optimal vaccination outcomes.

Vaccines containing epitopes which are short bits of immunogenic peptides, provide immunity, while recombinant vaccine technology utilizes complete genomes or big proteins. Therefore, this approach is incapable of inducing any allergic response in the recipient (36, 37).

The polytope vaccine offers several benefits over single-epitope and traditional vaccines because of its unique features. First, it incorporates multiple MHC epitopes, which allows recognition by various T-cell receptors. Second, it features overlapping CTL and T helper epitopes that activate innate and adaptive immune responses. Third, it contains poly epitopes from critical virulent antigens. Finally, it includes an immunostimulatory component to induce a sustained immune response. The development of this vaccine is increasingly significant, as it has shown the capacity to produce immunity in *in-vivo* experiments and has advanced to clinical trials (38).

This study employed various immune filters to identify specific sequences' epitopes (B cell, CTL, and Th). The applied filters required the epitope to possess promiscuous, antigenic, and immunogenic characteristics while lacking allergenic features. Additionally, the epitope needed to exhibit 100% conservation among target proteins and avoid overlapping with proteins in the human proteome. An appropriate vaccination was created based on epitopes and linked with a linker after conducting multiple immunoassays. Furthermore, the sequence was modified by including linkers KK, GPGPG, and AAY which effectively hindered the development of B cell, Th, and CTL binding epitopes. Utilizing specific sequences, such as linkers, helps enhance vaccine development. Prior research has consistently demonstrated that including KK, GPGPG, and AAY linkers among the B cell, Th, and CTL epitope sequences, respectively, enhances the binding immunogenicity. This leads to the development of a diverse range of vaccines with a streamlined design and building process (39-44). Bazhan *et al.* utilized comparable immunoinformatic methodologies to develop a vaccine targeting the Ebola virus. The researchers employed the IEDB database to forecast probable epitopes and created a vaccine that demonstrated immunogenicity when administered to animals (44).

Allergenicity is a significant concern in vaccine development, making it crucial to assess the allergenic characteristics of epitopes in the early stages of vaccine development. The epitopes selected for the vaccine design were based on their non-allergenic properties (45). The antigenic properties of each epitope were assessed using the VaxiJen v2.0 program, which is widely recognized as a reliable and consistent method for evaluating the antigenicity of proteins. VaxiJen v2.0 is a standalone alignment technique employed in reverse vaccinology to forecast antigens originating from viruses, bacteria, and tumors. The efficacy of this method was confirmed using internal training and external testing datasets, with the validation accuracy ranging from 70% to 89% (21). Several research utilized the VaxiJen tool and suggested that the proteins of SARS-CoV-2 have the most promising potential as vaccine candidates (46,47).

The vaccine designs' physicochemical characteristics were evaluated using ExPASy (48). In this study epitopes linked with appropriate connectors were evaluated for their stability based on antigenicity, allergenicity, toxicity, and physicochemical properties. The VaxiJen score demonstrated moderate antigenicity for Poly1 and slightly lower for Poly2, both were non-allergenic and non-toxic, making them viable vaccine candidates. Stability tests showed that Poly1 was less stable in mammalian systems but maintained longer stability in yeast and *E. coli*. Poly2, although less stable in yeast, was more stable in *E. coli* and showed superior thermostability overall, indicated by a lower instability index and higher aliphatic index. Their solubility characteristics, influenced by their grand average of hydropathy indices, are critical for vaccine formulation, with Poly1 being more hydrophilic and Poly2 slightly hydrophobic. The physicochemical qualities of vaccines are crucial in defining their stability, solubility, and immunogenicity, which are essential for ensuring their effectiveness and safety (49). Recent research, including our own, highlights the significance of these characteristics in the production of vaccines (50-52).

The desired epitopes that are expressed in the cytoplasm of cells can be detected by mouse MHC class I and II. Molecular docking was conducted to analyze the interaction between the peptides and the immune receptors, including MHCI and MHCII. The process of flexible docking utilizing the GalaxyPepDock server entails choosing the most favorable models based on the greatest scores of interaction similarity. Using the GalaxyPepDock server for flexible docking plays a vital role in clarifying the intricacies of peptide-MHC compatibility, which is essential for formulating successful vaccines. This finding aligns with the outcomes of the study conducted by Kardani *et al.* in which similar docking methods were utilized to evaluate the interactions between human immunodeficiency viruses (HIV-1) accessory proteins and MHC molecules. They, in particular, focused on interaction similarity scores to assess binding affinities (53). Consistent with other studies, our research specifically targeted many crucial proteins of SARS-CoV-2. The proteins that are part of the structure of the virus include the spike, nucleocapsid, membrane, and envelope proteins. In addition, much research has been conducted on many nonstructural proteins having significant functions in the viral lifecycle and pathogenicity (54-60). Nevertheless, our study takes a further step by employing dependable laboratory and clinical protocols to ascertain the safety and effectiveness of immunization. The technique utilized in this research differs from studies that exclusively depend on computational predictions by incorporating experimental validation ensuring the resilience and reproducibility of the conclusions. In the current study, ELISA and IFN-γ assays were utilized in mice to assess the immunological response triggered by the vaccination. The antibody levels in the serum of vaccinated mice were measured using ELISA testing, which offered valuable information on the humoral immune response. IFN-γ tests were employed to evaluate the cellular immunological response by quantifying the production of interferon-gamma, which is a crucial cytokine in the immune system's defense against viruses. These thorough assessments enable us to verify

not just the ability of the vaccine candidate to provoke an immune response, but also its effectiveness in providing protection. Our study combines evaluations of both humoral and cellular immunity to offer a comprehensive perspective on the vaccine's ability to give protection against SARS-CoV-2. This twofold strategy guarantees that the vaccination triggers a complete and efficient immune response, capable of neutralizing the pathogen and offering lasting protection.

The study conducted by Shafiee *et al*. was to create a new type of diphtheria vaccination by generating the recombinant protein DT386 in the *E. coli*. B-cell epitope prediction using BCEPred and T-cell epitope prediction using EpiJen were performed for the DT386 protein. BCEpred was used for B-cell epitopes with a 20-residue length and 75% specificity. EpiJen v1.0 was used for T-cell epitopes by inputting the protein sequence and selecting HLA*0101 as the allele before submitting the request. Then after, protein expression using SDS-PAGE and western blot analysis was confirmed (61). Far from this study in our investigation epitopes with high antigenicity, devoid of allergenicity and toxicity, were carefully chosen and then connected to create poly epitopes. The poly epitopes were produced in phage vectors and their 3D architectures were forecasted and improved utilizing bioinformatics servers.

Phage-based vaccines have gained popularity in recent years due to their inexpensive production costs, ease of preparation and genetic modification, capacity to be produced on a large scale, adjuvant capabilities, high stability at high-temperature settings, and wide variety of applications. Medical applications have taken into account the broad pH range, resilience to proteolytic and nucleolytic enzymes, and ability to withstand drying (62,63). Poly epitopes of the coronavirus' structural proteins spike, envelope, membrane, nucleocapsid, PLP, and RDRP were expressed on phage M13 in this study. *E. coli* host selection was employed to fuse these poly epitopes with protein pIII and convert them to nucleotide sequences. PHEN4 cloning was then outsourced to GeneCust. This approach involved transducing pM13ΔIII plasmids with pHEN4-Poly1 and pHEN4-Poly2 into *E. coli TG1* cells. The resulting phages displayed only recombinant protein III on their surface. The phage titer was measured at 10^{13} following purification by serial dilution. This ensures concentration of phage consistency for future studies. After phage immunization, animals' humoral immune responses were measured by ELISA. Serum OD increased significantly in recombinant phage-treated mice compared to controls. An immunological response in the form of phage antibodies is suggested. Assessing IFN-γ levels measured cellular immune responses. Subcutaneous phage injections increased IFN-γ levels compared to control groups, suggesting cellular immunity. The vaccine administered *via* gavage yielded similar outcomes. However cellular immunity response was not desirable because there was not significant response to lysate in recombinant phage group. Recombinant phages can induce humoral immune responses as seen by a significant increase in serum OD. The observation of elevated IFN-γ levels shows that phage transmission stimulated cellular immunological response, supporting the immunomodulatory properties of recombinant phages. The conducted preclinical investigations confirmed the immunogenicity of phage-based SARS-CoV-2 vaccines (64,65). The former noticed specific immune responses in mice, while the latter observed significant levels of anti-S antibodies and functional antibodies in baboons. The results align with the immunogenicity of other SARS-CoV-2 vaccine candidates, such as Ad26.COV2.S, has also demonstrated the capacity to induce strong humoral and cellular immune responses in animal models (66).

CONCLUSION

The global SARS-CoV-2 epidemic has been caused by SARS-CoV-2. Nevertheless, the approach to address SARS-CoV-2 quickly descended into a state of extreme chaos, rendering the situation uncontrollable. A vaccine candidate against this lethal virus was designed using an immunoinformatics technique. In the current study, a vaccine using B cell, CTL, and helper T lymphocyte epitopes derived from the viral proteins was designed

and developed. The vaccine exhibits both antigenic and immunogenic properties and has demonstrated a robust affinity for MHCI and MHCII based on molecular docking experiments. This study demonstrated that poly epitope-displaying phages, including antigenic epitopes of the SARS-CoV-2 virus, can effectively stimulate the humoral immune system in both administration routes (subcutaneous injection and gavage).

Acknowledgments

This study was performed at the Department of Genetics and Molecular Biology, School of Medicine, Isfahan University of Medical Sciences, Isfahan, Iran, with the grant gifted by Iran National Science Foundation (Grant No. 99007936). Additionally, financial support from Behyar Zist Company was utilized in this project. The results reported in this article are part of a Ph.D. thesis under the Correspond author's supervision.

Conflict of interest statement

The authors declared no competing interests in this study.

Authors' contributions

Sh. Mohammad Hasani contributed to the experimental design, performed the immunoinformatics analysis, and wrote the initial draft of the manuscript; M. Behdani was responsible for overseeing the experimental procedures, including the cloning and expression of the recombinant proteins, and provided critical revisions to the manuscript; Z. Amirkhani carried out the *in-vivo* studies, including mouse immunization and sample collection, and contributed to data analysis; I. Rahimmanesh assisted with the bioinformatics predictions and the selection of B and T cell epitopes; M. Esmaeilifallah cooperated in the preparation and purification of recombinant phages and conducted the ELISA assays to assess immune responses; E. Zaker contributed to writing the initial draft of the manuscript and assisted with the bioinformatics predictions and the selection of B and T cell epitopes. P. Nikpour assisted with reviewing the manuscript for grammatical and typographical errors; M. Fadaie participated in the design of the study and provided technical support throughout the experimental work; E. Ghafouri carried out the in-vivo studies, including mouse immunization and sample collection, and contributed to data analysis; Sh Naderi carried out the *in-vivo* studies and has contribution in the preparation and purification of recombinant phages; and H. Khanahmad supervised the overall project, provided guidance on the experimental design, and finalized the manuscript for submission. All authors read and approved the finalized article.

REFERENCES

1. Ullah M, Wahab A, Saeed S, Khan SU, Ali H, Humayun S, *et al*. Coronavirus and its terrifying inning around the globe: the pharmaceutical cares at the main frontline. Chemosphere. 2021;275:129968,1-14. DOI: 10.1016/j.chemosphere.2021.129968.
2. Wang Y, Wang Y, Chen Y, Qin Q. Unique epidemiological and clinical features of the emerging 2019 novel coronavirus pneumonia (COVID-19) implicate special control measures. J Med Virol. 2020;92(6):568-576. DOI: 10.1002/jmv.25748.
3. Niu S, Tian S, Lou J, Kang X, Zhang L, Lian H, *et al*. Clinical characteristics of older patients infected with COVID-19: a descriptive study. Arch Gerontol Geriatr. 2020;89:104058,1-6. DOI: 10.1016/j.archger.2020.104058.
4. Munster VJ, Koopmans M, Van Doremalen N, Van Riel D, de Wit E. A novel coronavirus emerging in China-key questions for impact assessment. N Engl J Med. 2020;382(8):692-694. DOI: 10.1056/NEJMp2000929.
5. ElBagoury M, Tolba MM, Nasser HA, Jabbar A, Elagouz AM, Aktham Y, *et al*. The find of COVID-19 vaccine: challenges and opportunities. J Infect Public Health. 2021;14(3):389-416. DOI: 10.1016/j.jiph.2020.12.025.
6. Liang S, Liu X, Zhang S, Li M, Zhang Q, Chen J. Binding mechanism of inhibitors to SARS-CoV-2 main protease deciphered by multiple replica molecular dynamics simulations. Phys Chem Chem Phys 2022;24(3):1743-1759. DOI: 10.1039/D1CP04361G.
7. Iacobucci G. Covid-19: new UK variant may be linked to increased death rate, early data indicate. BMJ. 2021;372(230):n230,1-2. DOI: 10.1136/bmj.n230.
8. Shariare MH, Parvez MAK, Karikas GA, Kazi M. The growing complexity of COVID-19 drug and vaccine candidates: challenges and critical transitions. J Infect Public Health. 2021;14(2): 214-220. DOI: 10.1016%2Fj.jiph.2020.12.009.

9. Francis MJ. Recent advances in vaccine technologies. Vet Clin North Am Small Anim Pract. 2018;48(2):231-241. DOI: 10.1016/j.cvsm.2017.10.002.
10. Mendoza-Ramírez NJ, García-Cordero J, Shrivastava G, Cedillo-Barrón L. The key to increase immunogenicity of next-generation COVID-19 vaccines lies in the inclusion of the SARS-CoV-2 nucleocapsid protein. J Immunol Res. 2024;2024(1):9313267,1-18. DOI: 10.1155/2024/9313267.
11. Grifoni A, Sidney J, Zhang Y, Scheuermann RH, Peters B, Sette A. A sequence homology and bioinformatic approach can predict candidate targets for immune responses to SARS-CoV-2. Cell Host Microbe. 2020;27(4):671-680.e2. DOI: 10.1016/j.chom.2020.03.002.
12. Ahmad S, Navid A, Farid R, Abbas G, Ahmad F, Zaman N, *et al*. Design of a novel multi epitope-based vaccine for pandemic coronavirus disease (COVID-19) by vaccinomics and probable prevention strategy against avenging zoonotics. Eur J Pharm Sci. 2020;151:105387, 1-16. DOI: 10.1016/j.ejps.2020.105387.
13. Bhattacharya M, Sharma AR, Patra P, Ghosh P, Sharma G, Patra BC, *et al.* Development of epitope-based peptide vaccine against novel coronavirus 2019 (SARS-COV-2): immunoinformatics approach. J Med Virol. 2020;92(6):618-631. DOI: 10.1002/jmv.25736.
14. Abdelmageed MI, Abdelmoneim AH, Mustafa MI, Elfadol NM, Murshed NS, Shantier SW, *et al*. Design of a multiepitope-based peptide vaccine against the E protein of human COVID-19: an immunoinformatics approach. Biomed Res Int. 2020;2020:1-12. DOI: 10.1155/2020/2683286.
15. van Houten NE, Henry KA, Smith GP, Scott JK. Engineering filamentous phage carriers to improve focusing of antibody responses against peptides. Vaccine. 2010;28(10):2174-2185. DOI: 10.1016/j.vaccine.2009.12.059.
16. Hess KL, Jewell CM. Phage display as a tool for vaccine and immunotherapy development. Bioeng Transl Med. 2020;5(1):e10142,1-15. DOI: 10.1002/btm2.10142.
17. Guan P, Doytchinova IA, Zygouri C, Flower DR. MHCPred: bringing a quantitative dimension to the online prediction of MHC binding. Appl Bioinformatics. 2003;2(1):63-66. PMID: 15130834.
18. Reynisson B, Barra C, Kaabinejadian S, Hildebrand WH, Peters B, Nielsen M. Improved prediction of MHC II antigen presentation through integration and motif deconvolution of mass spectrometry MHC eluted ligand data. J Proteome Res. 2020;19(6): 2304-2315. DOI: 10.1021/acs.jproteome.9b00874.
19. Saha S, Raghava GPS. Prediction of continuous B-cell epitopes in an antigen using recurrent neural network. Proteins. 2006;65(1):40-48. DOI: 10.1002/prot.21078.
20. Saha S, Raghava GPS, editors. BcePred: prediction of continuous B-cell epitopes in antigenic sequences using physico-chemical properties. Artif Intel Res.2004;3239:1-2.
21. Doytchinova IA, Flower DR. VaxiJen: a server for prediction of protective antigens, tumour antigens and subunit vaccines. BMC Bioinformatics. 2007;8(1):4,1-7. DOI: 10.1186/1471-2105-8-4.
22. Dimitrov I, Bangov I, Flower DR, Doytchinova I. AllerTOP v.2--a server for *in silico* prediction of allergens. J Mol Model. 2014;20(6):2278,1-6. DOI: 10.1007/s00894-014-2278-5.
23. Gupta S, Kapoor P, Chaudhary K, Gautam A, Kumar R. *In silico* approach for predicting toxicity of peptides and proteins. PloS One. 2013;8(9):e73957,1-10. DOI: 10.1371/journal.pone.0073957.
24. Buchan DW, Jones DT. The PSIPRED protein analysis workbench: 20 years on. Nucleic Acids Res. 2019;47(W1):W402-W407. DOI: 10.1093/nar/gkz297.
25. Gasteiger E, Hoogland C, Gattiker A, Duvaud S, Wilkins MR, Appel RD, *et al*. Protein identification and analysis tools on the ExPASy server. Springer.2005;571-607. DOI: 10.1385/1-59259-890-0:571.
26. Zhou X, Zheng W, Li Y, Pearce R, Zhang C, Bell EW, *et al*. I-TASSER-MTD: a deep-learning-based platform for multi-domain protein structure and function prediction. Nat Protoc. 2022;17(10):2326-2353. DOI: 10.1038/s41596-022-00728-0.
27. Heo L, Park H, Seok C. GalaxyRefine: protein structure refinement driven by side-chain repacking. Nucleic Acids Res. 2013;41(W1):W384-W388. DOI: 10.1093/nar/gkt458.
28. Lee H, Heo L, Lee MS, Seok C. GalaxyPepDock: a protein-peptide docking tool based on interaction similarity and energy optimization. Nucleic Acids Res. 2015;43(W1):W431-W435. DOI: 10.1093/nar/gkv495.
29. Stothard P. The sequence manipulation suite: JavaScript programs for analyzing and formatting protein and DNA sequences. Biotechniques. 2000;28(6):1102,1-2. DOI: 10.2144/00286ir01.
30. Grote A, Hiller K, Scheer M, Münch R, Nörtemann B, Hempel DC, *et al*. JCat: a novel tool to adapt codon usage of a target gene to its potential expression host. Nucleic Acids Res. 2005;33(suppl_2):W526-W531. DOI: 10.1093/nar/gki376.
31. Tjhung KF, Deiss F, Tran J, Chou Y, Derda R. Intra-domain phage display (ID-PhD) of peptides and protein mini-domains censored from canonical pIII phage display. Front Microbiol. 2015;6:340,1-11. DOI: 10.3389/fmicb.2015.00340.
32. Nakata Y, Tang X, Yokoyama KK. Preparation of competent cells for high-efficiency plasmid transformation of *Escherichia coli*. In: Cowell IG, Austin CA, editors. cDNA Libr Protoc. 1997. pp. 129-137. DOI: 10.1385/0-89603-383-X:129

33. Morse JS, Lalonde T, Xu S, Liu WR. Learning from the past: possible urgent prevention and treatment options for severe acute respiratory infections caused by 2019-nCoV. Chembiochem. 2020;21(5):730-738. DOI: 10.1002/cbic.202000047.
34. Srivastava S, Kamthania M, Pandey RK, Saxena AK, Saxena V, Singh SK, *et al*. Design of novel multi-epitope vaccines against severe acute respiratory syndrome validated through multistage molecular interaction and dynamics. J Biomol Struct Dyn. 2019;37(16):4345-4360. DOI: 10.1080/07391102.2018.1548977.
35. Chauhan V, Rungta T, Goyal K, Singh MP. Designing a multi-epitope based vaccine to combat kaposi sarcoma utilizing immunoinformatics approach. Sci Rep. 2019;9(1):2517,1-15. DOI: 10.1038/s41598-019-39299-8.
36. Shoari A, Khodabakhsh F, Ahangari Cohan R, Salimian M, Karami E. Anti-angiogenic peptides application in cancer therapy; a review. Res Pharm Sci. 2021;16(6):559-574. DOI: 10.4103/1735-5362.327503.
37. He R, Yang X, Liu C, Chen X, Wang L, Xiao M, *et al*. Efficient control of chronic LCMV infection by a CD4 T cell epitope-based heterologous prime-boost vaccination in a murine model. Cell Mol Immunol. 2018;15(9):815-826. DOI: 10.1038/cmi.2017.3.
38. Zheng Y, He R, He M, Gu X, Wang T, Lai W, *et al*. Characterization of Sarcoptes scabiei cofilin gene and assessment of recombinant cofilin protein as an antigen in indirect-ELISA for diagnosis. BMC Infect Dis. 2015;16(1):1-7. DOI: 10.1186/s12879-016-1353-1.
39. Hou J, Liu Y, Hsi J, Wang H, Tao R, Shao Y. Cholera toxin B subunit acts as a potent systemic adjuvant for HIV-1 DNA vaccination intramuscularly in mice. Hum Vaccin Immunother. 2014;10(5):1274-1283. DOI: 10.4161/hv.28371.
40. Kim HJ, Kim J-K, Seo SB, Lee HJ, Kim H-J. Intranasal vaccination with peptides and cholera toxin subunit B as adjuvant to enhance mucosal and systemic immunity to respiratory syncytial virus. Arch Pharm Res. 2007;30(3):366-371. DOI: 10.1007/BF02977620.
41. Tamura S, Funato H, Nagamine T, Aizawa C, Kurata T. Effectiveness of cholera toxin B subunit as an adjuvant for nasal influenza vaccination despite pre-existing immunity to CTB. Vaccine. 1989;7(6):503-505. DOI: 10.1016/0264-410x(89)90273-9.
42. Meza B, Ascencio F, Sierra-Beltrán AP, Torres J, Angulo C. A novel design of a multi-antigenic, multistage and multi-epitope vaccine against *Helicobacter pylori*: an *in silico* approach. Infect Genet Evol. 2017;49:309-317. DOI: 10.1016/j.meegid.2017.02.007.
43. Khatoon N, Pandey RK, Prajapati VK. Exploring *Leishmania secretory* proteins to design B and T cell multi-epitope subunit vaccine using immunoinformatics approach. Sci Rep. 2017;7(1):8285,1-12. DOI: 10.1038/s41598-017-08842-w.
44. Bazhan SI, Antonets DV, Karpenko LI, Oreshkova SF, Kaplina ON, Starostina EV, *et al*. *In silico* designed Ebola virus T-cell multi-epitope DNA vaccine constructions are immunogenic in mice. Vaccines. 2019;7(2):34,1-15. DOI: 10.3390/vaccines7020034.
45. Saha S, Raghava GPS. AlgPred: prediction of allergenic proteins and mapping of IgE epitopes. Nucleic Acids Res. 2006;34(suppl_2):W202-W209. DOI: 10.1093/nar/gkl343.
46. Ong E, Wong MU, Huffman A, He Y. COVID-19 coronavirus vaccine design using reverse vaccinology and machine learning. Front immunol. 2020;11:1581,1-13. DOI: 10.3389/fimmu.2020.01581.
47. Huffman A, Ong E, Hur J, D'Mello A, Tettelin H, He Y. COVID-19 vaccine design using reverse and structural vaccinology, ontology-based literature mining and machine learning. Brief Bioinform 2022;23(4):1-16. DOI: 10.1093/bib/bbac190.
48. Walker JM. The proteomics protocols handbook: Springer; 2005. pp. 571-607. DOI: 10.1385/1592598900.
49. Dey AK, Malyala P, Singh M. Physicochemical and functional characterization of vaccine antigens and adjuvants. Expert Rev Vaccines. 2014;13(5): 671-685. DOI: 10.1586/14760584.2014.907528.
50. Rowaiye AB, Oli AN, Asala MT, Nwonu EJ, Njoku MO, Asala OO, *et al*. Design of multiepitope vaccine candidate from a major capsid protein of the African swine fever virus. Vet Vaccine. 2023;2(1):100013, 1-15. DOI: 10.1016/j.vetvac.2023.100013.
51. Almofti YA, Abd-Elrahman KA, Eltilib EE. Vaccinomic approach for novel multi epitopes vaccine against severe acute respiratory syndrome coronavirus-2 (SARS-CoV-2). BMC Immunol. 2021;22:1-20. DOI: 10.1186/s12865-021-00412-0.
52. Mehrab R, Sedighian H, Sotoodehnejadnematalahi F, Halabian R, Fooladi AAI. A comparative study of the arazyme-based fusion proteins with various ligands for more effective targeting cancer therapy: an *in-silico* analysis. Res Pharm Sci. 2023;18(2):159-176. DOI: 10.4103/1735-5362.367795.
53. Kardani K, Hashemi A, Bolhassani A. Comparison of HIV-1 Vif and Vpu accessory proteins for delivery of polyepitope constructs harboring Nef, Gp160 and P24 using various cell penetrating peptides. PLoS One. 2019;14(10):e0223844,1-28. DOI: 10.1371/journal.pone.0223844.
54. Khan MT, Islam MJ, Parihar A, Islam R, Jerin TJ, Dhote R, *et al.* Immunoinformatics and molecular modeling approach to design universal multi-epitope vaccine for SARS-CoV-2. Inform Med Unlocked. 2021;24:100578,1-12. DOI: 10.1016/j.imu.2021.100578.
55. Rasheed MA, Raza S, Zohaib A, Riaz MI, Amin A, Awais M, *et al.* Immunoinformatics based prediction of recombinant multi-epitope vaccine for the control

and prevention of SARS-CoV-2. Alex Eng J. 2021;60(3):3087-3097.
DOI: 10.1016/j.aej.2021.01.046.
56. Naveed M, Tehreem S, Arshad S, Bukhari SA, Shabbir MA, Essa R, *et al*. Design of a novel multiple epitope-based vaccine: an immunoinformatics approach to combat SARS-CoV-2 strains. J Infect Public Health. 2021;14(7):938-946.
DOI: 10.1016/j.jiph.2021.04.010.
57. Joshi A, Joshi BC, Mannan MA, Kaushik V. Epitope based vaccine prediction for SARS-COV-2 by deploying immuno-informatics approach. Inform Med Unlocked. 2020;19:100338,1-10.
DOI: 10.1016/j.imu.2020.100338.
58. Sarkar B, Ullah MA, Araf Y, Rahman MS. Engineering a novel subunit vaccine against SARS-CoV-2 by exploring immunoinformatics approach. Inform Med Unlocked. 2020;21:100478,1-18.
DOI: 10.1016/j.imu.2020.100478.
59. Bashir Z, Ahmad SU, Kiani BH, Jan Z, Khan N, Khan U, *et al.* Immunoinformatics approaches to explore B and T cell epitope-based vaccine designing for SARS-CoV-2 Virus. Pak J Pharm Sci. 2021;34(1):345-352.
PMID: 34275860.
60. Oliveira SC, de Magalhaes MT, Homan EJ. Immunoinformatic analysis of SARS-CoV-2 nucleocapsid protein and identification of COVID-19 vaccine targets. Front Immunol. 2020;11:587615, 1-10.
DOI: 10.3389/fimmu.2020.587615.
61. Shafiee F, Rabbani M, Behdani M, Jahanian-Najafabadi A. Expression and purification of truncated diphtheria toxin, DT386, in *Escherichia coli*: an attempt for production of a new vaccine against diphtheria. Res Pharm Sci. 2016;11(5):428-434.
DOI: 10.4103/1735-5362.192496.
62. González-Mora A, Hernández-Pérez J, Iqbal HM, Rito-Palomares M, Benavides J. Bacteriophage-based vaccines: a potent approach for antigen delivery. Vaccines. 2020;8(3):504,1-24.
DOI: 10.3390/vaccines8030504.
63. Ghajavand H, Esfahani BN, Havaei A, Fazeli H, Jafari R, Moghim S. Isolation of bacteriophages against multidrug resistant *Acinetobacter baumannii*. Res Pharm Sci. 2017;12(5):373-380.
DOI: 10.4103/1735-5362.213982.
64. Staquicini DI, Tang FH, Markosian C, Yao VJ, Staquicini FI, Dodero-Rojas E, *et al*. Design and proof of concept for targeted phage-based COVID-19 vaccination strategies with a streamlined cold-free supply chain. Proc Natl Acad Sci U S A. 2021;118(30):e2105739118,1-9.
DOI: 10.1073/pnas.2105739118.
65. Tian JH, Patel N, Haupt R, Zhou H, Weston S, Hammond H, *et al*. SARS-CoV-2 spike glycoprotein vaccine candidate NVX-CoV2373 immunogenicity in baboons and protection in mice. Nat Commun. 2021;12(1):372,1-14.
DOI: 10.1038/s41467-020-20653-8.
66. Bos R, Rutten L, van der Lubbe JE, Bakkers MJ, Hardenberg G, Wegmann F, *et al*. Ad26 vector-based COVID-19 vaccine encoding a prefusion-stabilized SARS-CoV-2 Spike immunogen induces potent humoral and cellular immune responses. NPJ Vaccines. 2020;5(1):91,1-11.
DOI: 10.1038/s41541-020-00243-x.